General Disclaimer

One or more of the Following Statements may affect this Document

- This document has been reproduced from the best copy furnished by the organizational source. It is being released in the interest of making available as much information as possible.

- This document may contain data, which exceeds the sheet parameters. It was furnished in this condition by the organizational source and is the best copy available.

- This document may contain tone-on-tone or color graphs, charts and/or pictures, which have been reproduced in black and white.

- This document is paginated as submitted by the original source.

- Portions of this document are not fully legible due to the historical nature of some of the material. However, it is the best reproduction available from the original submission.

NASA TECHNICAL MEMORANDUM

NASA TM X-73563

NASA TM X-73563

ANALYSIS OF EPITAXIAL DRIFT FIELD N ON P SILICON SOLAR CELLS

by Cosmo R. Baraona and Henry W. Brandhorst, Jr.
Lewis Research Center
Cleveland, Ohio 44135

TECHNICAL PAPER to be presented at the
Twelfth Photovoltaic Specialists Conference sponsored by the
Institute of Electrical and Electronics Engineers
Baton Rouge, Louisiana, November 15-18, 1976

ANALYSIS OF EPITAXIAL DRIFT FIELD N ON P SILICON SOLAR CELLS

Cosmo R. Baraona and Henry W. Brandhorst, Jr.
National Aeronautics and Space Administration
Lewis Research Center
Cleveland, Ohio 44135

SUMMARY

Performance of epitaxial drift field silicon solar cell structures having a variety of impurity profiles has been calculated. These structures consist of a uniformly doped P-type substrate layer, and a P-type epitaxial drift field layer with a variety of field strengths. Several N-layer structures were modeled. A four layer solar cell model was used to calculate efficiency, open circuit voltage and short circuit current. The effect on performance of layer thickness, doping level, and diffusion length was determined. The results show that peak initial efficiency of 18.1% occurs for a drift field thickness of about 30 μm with the doping rising from 10^{17} atoms/cm^3 at the edge of the depletion region to 10^{18} atoms/cm^3 in the substrate. Stronger drift fields (narrow field regions) allowed very high performance (17% efficiency) even after irradiation to 3×10^{14} 1 MeV electrons/cm^2.

E-9007

INTRODUCTION

Methods of improving silicon solar cell performance include incorporating back surface fields (BSF) (1-4) and drift fields (DF) (5-7) into the structure. The back surface field is an abrupt (i.e., several orders of magnitude) doping level change in a short (i.e., a few microns) distance. The drift field solar cell is usually made by epitaxial deposition in which doping level changes occur over longer distances.

The epitaxial BSF cell has been reported previously (4). It was shown that the BSF can be made by epitaxial deposition, that the substrate diffusion length can influence performance and that low-high junction theory can be used to predict cell performance. Experimental results on epitaxial drift field structures have also been reported (5). It was shown that reproducible good quality junctions can be made. Intentionally graded epitaxial drift field layers resulted in high (0.636 V) open circuit voltages. While these results are promising, a more comprehensive evaluation of doping profiles and epitaxial layer thickness ranges is needed to pinpoint optimum structures. Because the number of possible combinations of cell construction features and materials properties is great, an experimental evaluation would be time consuming and expensive.

The present work explores analytically the performance of a wide range of epitaxial drift field N on P solar cell structures. The purpose is to identify the cell design feature producing highest performance. A four layer solar cell model was used in these calculations. This model has been used previously (8, 9) to calculate solar cell performance with good agreement with experiment. Cell performance calculated with this model includes short circuit current density, J_{sc}, open circuit voltage, V_{oc}, and efficiency. The influence on performance of field strength, substrate doping level, epitaxial layer width, diffusion length, and N-layer profile was determined. In all cases, the limits of present technology were used to determine achievable ranges and values for the modeling parameters so that the calculated performance would be realistic.

MODELING OF THE EPITAXIAL DRIFT FIELD CELL

Theoretical Model

The cell model used has been described elsewhere (8, 9). It is based on a four layer, homojunction semiconductor device in which region widths, impurity concentrations, and material properties such as diffusion length, mobility, and reflectivity can be specified. A schematic of the cell model is shown in Fig. 1. Only exponential impurity distributions are assumed, resulting in constant drift field strengths within each layer.

The model was derived by solving the continuity equation using the current transport equation and appropriate boundary conditions to solve for the diode saturation current density (J_0) and for J_{sc}. The V_{oc}, maximum power (P_{max}) and air mass zero (AMO) efficiency (eff) were calculated from the following expressions:

$$V_{oc} = \frac{kT}{q} \ln\left(\frac{J_{sc}}{J_0} + 1\right) \tag{1}$$

$$P_{max} = CF\, V_{oc}\, J_{sc} \tag{2}$$

$$EFF = \left(\frac{P_{max}}{135.3}\right) \times 100\% \tag{3}$$

where k is Boltzmann's constant, T is temperature, q is electronic charge, CF is curve factor which was calculated as previously described (8). The curve factor assumes unity diode quality factor (n = 1) and zero series resistance. For most cells, series resistance leads to about a 3% loss in power and curve factor. However, these data were not adjusted for that loss. The AMO solar constant used was 135.3 mW/cm^2.

Figure 2 shows the expected value of diffusion length as a function of doping level before radiation damage (10) and after a radiation fluence of 3×10^{14} 1 MeV electrons/cm^2 (end of life, EOL) (11). Even though doping level was assumed to vary exponentially in the epitaxial layer, only single values of diffusion length and mobility in each layer are possible

with the model used. The values chosen for modeling were based on the impurity concentration at the center of the epitaxial layer.

The four layer solar cell model has been used previously to calculate performance of epitaxial BSF cells (4), drift field lithium cells (8), and alloyed BSF cells (9). Agreement between calculated and experimental results was good. Thus extension of this model to the present study can be done with confidence.

P-Layer Data

The range of values for the doping level in the uniformly doped substrate, N_{sub}, and at the depletion region edge, N_{epi}, the width of the epitaxial layer, W_{epi}, and the diffusion length in the epitaxial layer, L_{epi}, are shown in Table I. The doping level combinations were constrained such that $N_{epi} \leq N_{sub}$. The field strength in the epitaxial layer, E_{epi}, can be calculated using these parameters and the equation

$$E_{epi} = \frac{kT}{qW_{epi}} \ln\left(\frac{N_{sub}}{N_{epi}}\right) \quad (4)$$

The order of magnitude difference between the N_{sub} and N_{epi} doping concentration is defined as:

$$\Delta = \log_{10} \frac{N_{sub}}{N_{epi}} \quad (5)$$

N-Layer Data

The principal criterion for the design of the N-layer is that it yield high conversion efficiency, high short wavelength (0.4 μm) collection efficiency, and high V_{oc}. There are a large number of N-layer constructions and an even larger number of possible P-layer configurations. In order to limit the number of calculations, guidelines were used to reduce the number of N-layer profiles evaluated to six.

These guidelines were that: (1) junction depth, X_j, be shallow ($\leq$1 μm) for good collection efficiency, (2) carrier concentrations be high for good V_{oc} but no higher than 10^{19} atoms/cm^3 to avoid heavy doping effects (13, 14), and (3) present epitaxial technology limits doping level changes to about two orders of magnitude and layer widths to a minimum of 1 micron. In addition, surface reflectivity of 3% (12) and a front surface recombination velocity of 10^3 cm/sec were used. A diffusion length of 3 μm was used in the N-layer. This value is comparable to those measured on bulk material doped to this level.

With these guidelines, the N-layer profiles shown in Fig. 3 were used in the calculations. The A and B profiles could be made by epitaxial deposition of a uniformly doped N-layer with subsequent diffusion of a more heavily doped, N-type profile. The C and D profiles are typical of those obtained by diffusion, however, a 0.25 μm layer thickness may be too thin for epitaxial deposition. These layers were included in the evaluation for comparison to more conventional N-layer profiles. The E and F profiles could be made by epitaxial deposition directly.

RESULTS AND DISCUSSION

N-Layer Effects

The sensitivity of cell performance to N-layer profile was investigated. Calculations were made for two P-layer profiles with each N-layer profile shown in Fig. 3. The P-layer profiles were $N_{sub} = 10^{18}$ cm^{-3}, $N_{epi} = 10^{17}$ cm^{-3}, and $N_{sub} = 10^{17}$ cm^{-3}, $N_{epi} = 10^{16}$ cm^{-3}.

Table II shows collection efficiency, V_{oc} and conversion efficiency for each N-layer profile. The performance is high even for the 1 micron junction depth profiles. This is due to the good N-layer parameters used and shows that shallow junctions are not needed if 3 μm diffusion length in the N-layer is achieved. Profiles C and D are less desirable because the 0.25 micron junction depth may not be attainable by epitaxial methods. Profiles A and B have somewhat lower performance than profile E. Note that although the difference in collection efficiency between C and E seems high, there is only 0.1 percent difference in efficiency. Although profile F has a higher collection efficiency (due to its higher field strength), the V_{oc} is lower because of the lower impurity concentration at the depletion region edge. This leads to a lower efficiency. Profile E has a high overall performance and can also be fabricated with existing epitaxial technology. Therefore, based on these results, profile E was used for the remaining calculations with the P-layer.

P-Layer Effects - Initial Performance

Using the expected values of L_{epi} shown in Fig. 2, each of the P-layer cases has a maximum efficiency at some value of N_{epi} and W_{epi}. The highest of these maxima (called the peak efficiency) for each value of N_{sub} is shown in Fig. 4. The $N_{sub} = 10^{18}$ cm^{-3} case has the best overall efficiency, 18.1%. For higher or lower values of N_{sub}, efficiency drops.

In Fig. 5, the importance of N_{epi} in achieving high efficiency is shown. Maximum efficiency for each case is plotted against N_{sub} with N_{epi} as a parameter. Note that Fig. 4 was derived from Fig. 5 by plotting the upper envelope of efficiency at each N_{sub} doping level. The overall highest efficiency, 18.1%, is for the $N_{sub} = 10^{18}$ cm^{-3}, $N_{epi} = 10^{17}$ cm^{-3}, $\Delta = 1$ case. The next closest efficiencies of about 17.8% are for the uniformly doped 10^{17} cm^{-3} and 10^{18} cm^{-3} cases. Thus these three cases define the area of greatest interest to the solar cell designer.

The uniformly doped 10^{17} cm^{-3} case gives the highest J_{sc} (43.8 mA/cm^2) because of its high diffusion length. The uniformly doped 10^{18} cm^{-3} case gives the highest V_{oc} (0.703 V) because of its high doping levels at the depletion region edge. However the efficiencies in these cases are

somewhat lower than the $N_{sub} = 10^{18}$ cm^{-3}, $N_{epi} = 10^{17}$ cm^{-3} case. This latter case is a better compromise between the uniformly doped cases because high voltage (0.671 V) is attained without significantly reducing J_{sc} (43.5 mA/cm^2). The doping level, diffusion length and drift field aided collection combine to give best performance in this case. Thus moderate drift fields do offer a performance advantage at beginning of life.

High doping level differences ($\Delta > 2$) are not an advantage. For example at $N_{sub} = 10^{19}$ cm^{-3}, the highest efficiency of 16.75% is for $N_{epi} = 10^{17}$ cm^{-3}, $\Delta = 2$. Higher values of doping level difference ($\Delta > 2$) do not result in the highest maximum efficiency. At $N_{sub} = 10^{19}$ cm^{-3}, maximum efficiency at $N_{epi} = 10^{16}$ cm^{-3}, $\Delta = 3$ is below that for the $N_{epi} = 10^{17}$ cm^{-3}, $\Delta = 2$ case.

Figure 5 also shows that for $N_{sub} \leq 10^{17}$ cm^{-3}, peak efficiency is for a nonfield, conventional cell, i.e., $N_{sub} = N_{epi}$, $\Delta = 0$. Thus for lightly doped substrates, the drift field epitaxial cell has no advantage. The V_{oc} achieved with high N_{epi} makes a greater contribution to performance than that due to the high field strengths which result from low N_{epi}.

Figure 6 shows the variation of efficiency with width of the epitaxial layer for the $N_{epi} = 10^{17}$ cm^{-3}, $N_{sub} = 10^{18}$ cm^{-3} and 10^{19} cm^{-3} cases. Maximum efficiency of 18.1% for $N_{sub} = 10^{18}$, $N_{epi} = 10^{17}$, $\Delta = 1$ case is at $W_{epi} \approx$ 30 microns. Equation (4) shows that this corresponds to a field strength of about 20 V/cm. This peak is due to a balance between increasing V_{oc} and decreasing J_{sc} as W_{epi} decreases. This effect is shown more fully in Fig. 7. These data are for the $N_{sub} = 10^{18}$ cm^{-3}, $N_{epi} = 10^{17}$ cm^{-3}, $\Delta = 1$ case. Maximum efficiency of 18.1% occurs at about $W_{epi} = 30$ microns. The increase of V_{oc} as W_{epi} decreases is due to increasing field strength and to the decrease of the ratio of W_{epi} to L_{epi}. This decreasing ratio leads to a decrease in the calculated reverse saturation current and thus increasing V_{oc}.

The effect of epitaxial layer diffusion length on efficiency for the $N_{sub} = 10^{18}$ cm^{-3}, $N_{epi} = 10^{17}$ cm^{-3} case is shown in Fig. 8. The 18.1% efficiency discussed above occurs at a $L_{epi} = 60$ μm value obtained from Fig. 2 for this substrate doping level. If epitaxial technology cannot produce material with this diffusion length, then peak efficiency will be reduced. Conversely, if epitaxial methods can produce higher diffusion length materials at these doping levels, higher peak efficiencies appear possible.

P-LAYER EFFECTS - END OF LIFE PERFORMANCE

In Fig. 9, peak efficiency is plotted against N_{sub} for the end of life (EOL) L_{epi} values shown in Fig. 2. The initial peak efficiency curve from Fig. 4 is included for reference. After a fluence of 3×10^{14} cm^{-2} the highest peak efficiency of 17.1% is still for the $N_{sub} = 10^{18}$ cm^{-3}, and $N_{epi} = 10^{17}$ cm^{-3} case. Higher and lower values of N_{sub} have EOL efficiencies below 17%.

Figure 10 shows efficiency against W_{epi} for the $N_{sub} = 10^{18}$ cm^{-3}, $N_{epi} = 10^{17}$ cm^{-3} case for several values of L_{epi}. The maximum efficiency point shifts from $W_{epi} = 30$ μm (field strength of 20 V/cm) to $W_{epi} \approx 8$ μm (field strength of 75 V/cm) as L_{epi} decreases. This shows the importance of field strength in achieving high EOL efficiencies. Note that the initial and EOL peak efficiency values do not occur for the same cell structure. However, by altering layer thickness to about 15 μm, a nearly optimum performance can be achieved. In this case, initial efficiency is about 18% while EOL efficiency is 17.1%. Another design choice would be to minimize decrease in performance with radiation fluence. In that case, an 8 μm thick layer would have an initial efficiency of 17.7% and an EOL efficiency of 17.2%.

CONCLUSIONS

The P-region doping levels of greatest interest to the solar cell designer have been identified as ranging between 10^{17} cm^{-3} and 10^{18} cm^{-3}. Within this range tradeoffs between V_{oc} and J_{sc} plus use of drift fields combine to give the highest efficiency. Drift fields slightly improve solar cell beginning of life performance within this range. A peak initial efficiency of 18.1% was calculated for the substrate doping level of 10^{18} cm^{-3}, epitaxial layer doping level of 10^{17} cm^{-3}, epitaxial layer width of 30 μm, field strength of 20 V/cm P-layer case. Diffusion length of 60 μm, the drift field and good solar cell properties combine to yield this efficiency.

High values of field strength in the epitaxial layer (i.e., above approximately 100 V/cm) do not result in the highest efficiencies. The cell structures that produced the highest efficiencies for substrate doping levels $\leq 10^{17}$ cm^{-3} were nonfield, uniformly doped structures. This is because the open circuit voltages achieved with high values of epitaxial layer doping level are greater than those obtained in the high field case where this value is necessarily low.

High collection efficiencies (i.e., above 0.95) and high conversion efficiencies are possible with deep (1 μm) junction depths if high (3 μm) diffusion lengths are assumed.

The highest efficiency for end of life (3×10^{14} e/cm^2) was 17.2%. This occurs for a substrate doping level of 10^{18} cm^{-3}, epitaxial layer doping level of 10^{17} cm^{-3}, and epitaxial layer width of 8 μm. Field strength is an important parameter for achieving high EOL efficiency. Thin epitaxial layers and high field strengths give the best EOL efficiencies. Change of W_{epi} to 15 μm results in near optimum initial and EOL performance. This yields a cell with initial efficiency of 18.0% and an EOL efficiency of 17.1%. This represents a tradeoff between highest initial and EOL efficiency.

REFERENCES

1. J. Mandelkorn and J. H. Lamneck, Jr., "Simplified Fabrication of Back Surface Electric Field Silicon Solar Cells and Novel Characteristics of Such Cells," NASA TM X-68060, May 1972.

2. P. A. Iles, "Increased Output from Silicon Solar Cells," Conference Record of the Eighth IEEE Photovoltaic Specialists Conference, Seattle, WA., p. 345, Aug. 1970.

3. H. Fischer, E. Link, and W. Pschunder, "Influence of Controlled Lifetime Doping on Ultimate Technological Performance of Silicon Solar Cells," Conference Record of the Eighth IEEE Photovoltaic Specialists Conference, Seattle, WA., p. 70, Aug. 1970.

4. H. W. Brandhorst, Jr., C. R. Baraona, and C. K. Swartz, "Performance of Epitaxial Back Surface Field Cells," Conference Record of the Tenth IEEE Photovoltaic Specialists Conference, Palo Alto, CA., Nov. 1973.

5. R. V. D'Aiello, P. H. Robinson, and H. Kressel, "Epitaxial Solar Cell Fabrication," NASA CR-134968, Dec. 1975.

6. K. S. Tarneja, R. K. Riel, V. A. Rossi, and E. R. Stonebraker, "Drift Field Dendritic Solar Cells." Proceedings of the Fifth IEEE Photovoltaic Specialists Conference, Greenbelt, MD., Vol. I, No. A-3, Oct. 1965.

7. P. M. Dunbar and J. R. Hauzer, "A Theoretical Analysis of the Current Voltage Characteristics of Solar Cells," pp. 63-78, NGR30-002-195, Aug. 1976.

8. M. P. Godlewski, C. R. Baraona, and H. W. Brandhorst, Jr., "The Drift Field Model Applied to the Lithium-Containing Silicon Solar Cell," Conference Record of the Tenth IEEE Photovoltaic Specialist Conference, Palo Alto, CA., Nov. 1973.

9. M. P. Godlewski, C. R. Baraona, and H. W. Brandhorst, Jr., "Low-High Junction Theory Applied to Solar Cells," Conference Record of the Tenth IEEE Photovoltaic Specialist Conference, Palo Alto, CA., Nov. 1973.

10. P. Iles, Optical Coating Labs, Inc., Private Communication.

11. J. R. Srour, S. Othmer, K. Y. Chiu, and O. L. Curtis, Jr., "Damage Coefficients in Low Resistivity Silicon," NASA CR-134768, May 1975.

12. C. R. Baraona and H. W. Brandhorst, Jr., "V-Grooved Silicon Solar Cells," Conference Record of the Eleventh Photovoltaic Specialists Conference, Phoenix, Ariz., May 1975.

13. M. P. Godlewski, H. W. Brandhorst, Jr., and C. R. Baraona, "Effects of High Doping Levels on Silicon Solar Cell Performance," Conference Record of the IEEE Photovoltaic Specialist Conference, Phoenix, Ariz., May 1975.

14. J. W. Slotboom and H. C. deGraff, "Experimental Determination of the Bandgap in the Base Region of Bipolar Transistors," International Electron Devices Meeting, IEEE Press, N. Y., 1975.

TABLE I. - RANGE OF PARAMETERS USED TO MODEL DRIFT FIELD SOLAR CELL

Parameter	Range
N_{sub}	10^{14} to 10^{19} atoms/cm^3
N_{epi}	10^{14} to 10^{19} atoms/cm^3
W_{epi}	8 to 178 μm
L_{epi}	10 to 100 μm
E_{epi}	0 to 372 V/cm
Δ	1 to 5

TABLE II. - SUMMARY OF PERFORMANCE OF CELL WITH DIFFERENT N-LAYER PROFILES

N-layer profile	Junction depth, μm	Collection efficiency, at 0.4 μm	V_{oc}, V	Efficiency, %
A	1	0.912	0.675	17.3
B	1	.944	.620	15.9
C	.25	.992	.691	18.1
D	.25	.996	.679	17.8
E	1	.958	.689	18.0
F	1	.979	.662	17.3

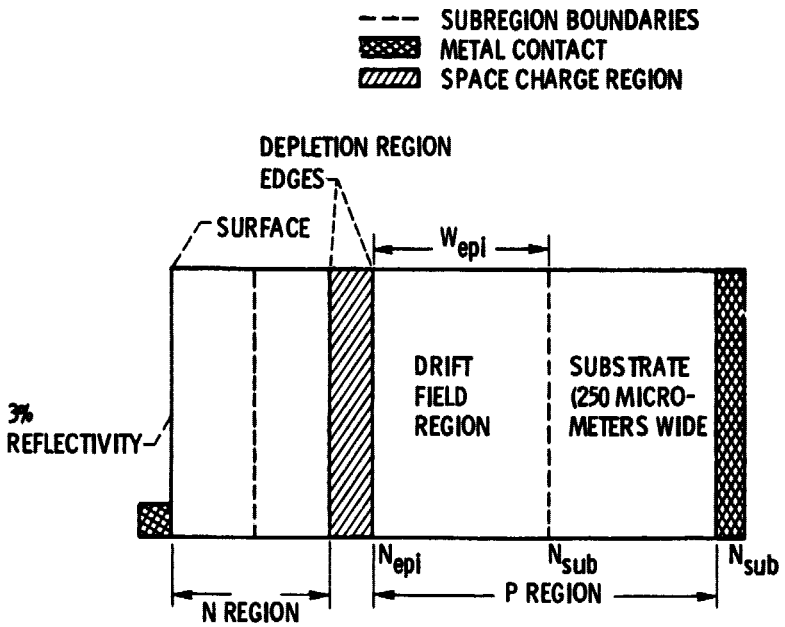

Figure 1. - Cross section of drift field cell model.

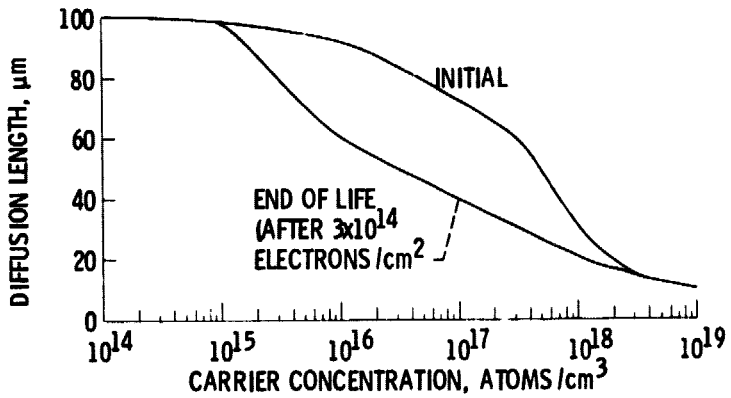

Figure 2. - Variation of diffusion length with carrier concentration before and after electron irradiation.

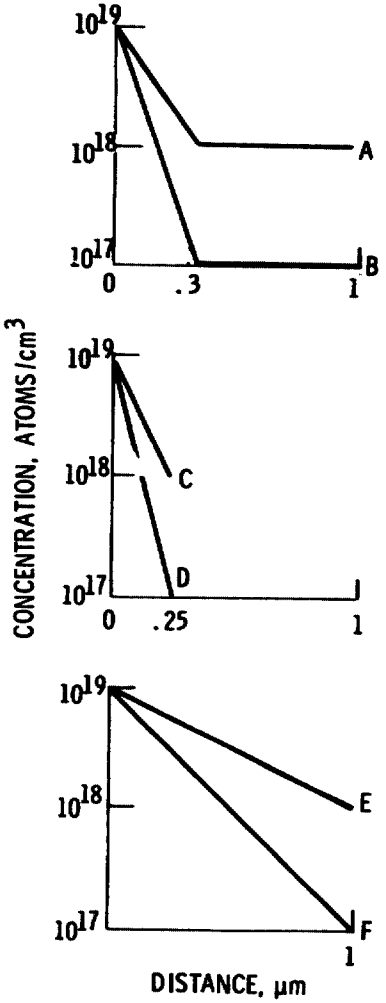

Figure 3. - Variation of N-layer carrier concentration with distance from illuminated surface (six cases considered in this study).

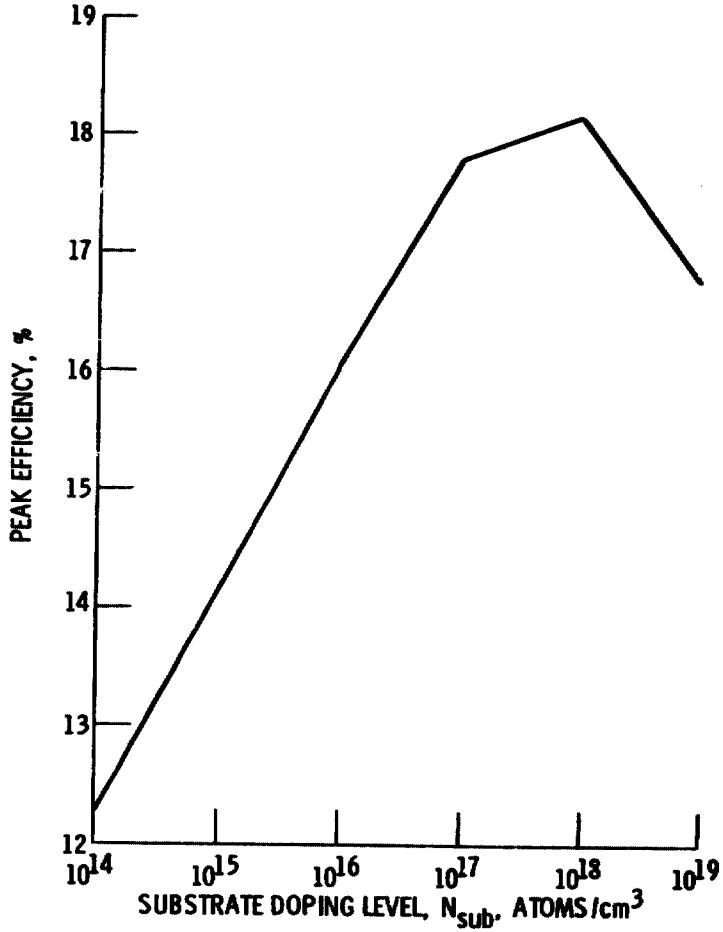

Figure 4. - Dependence of peak efficiency on substrate doping concentration.

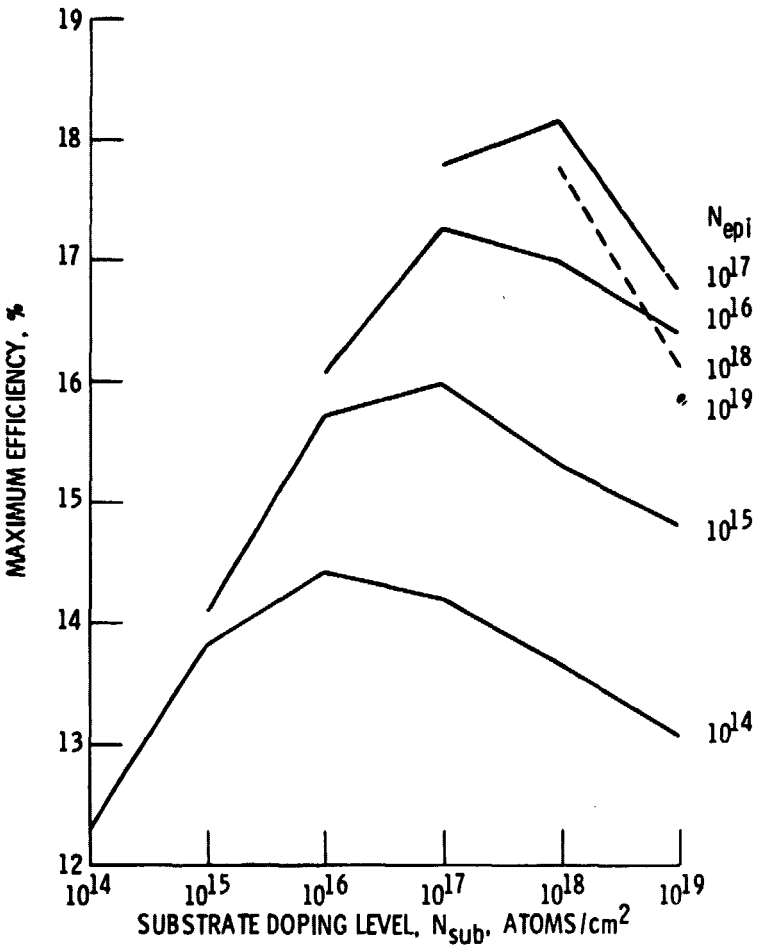

Figure 5. - Variation of maximum efficiency with substrate doping level for values of epitaxial level.

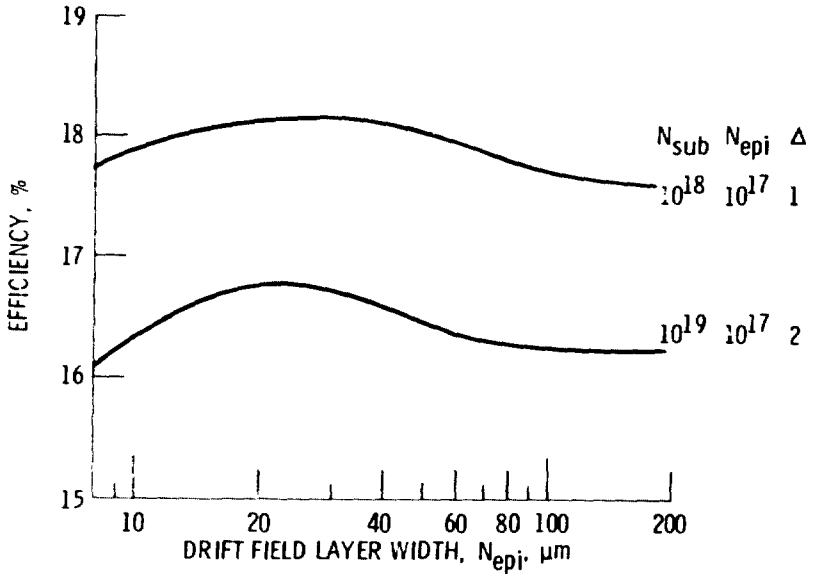

Figure 6. - Dependence of efficiency on drift field layer width for two doping level cases.

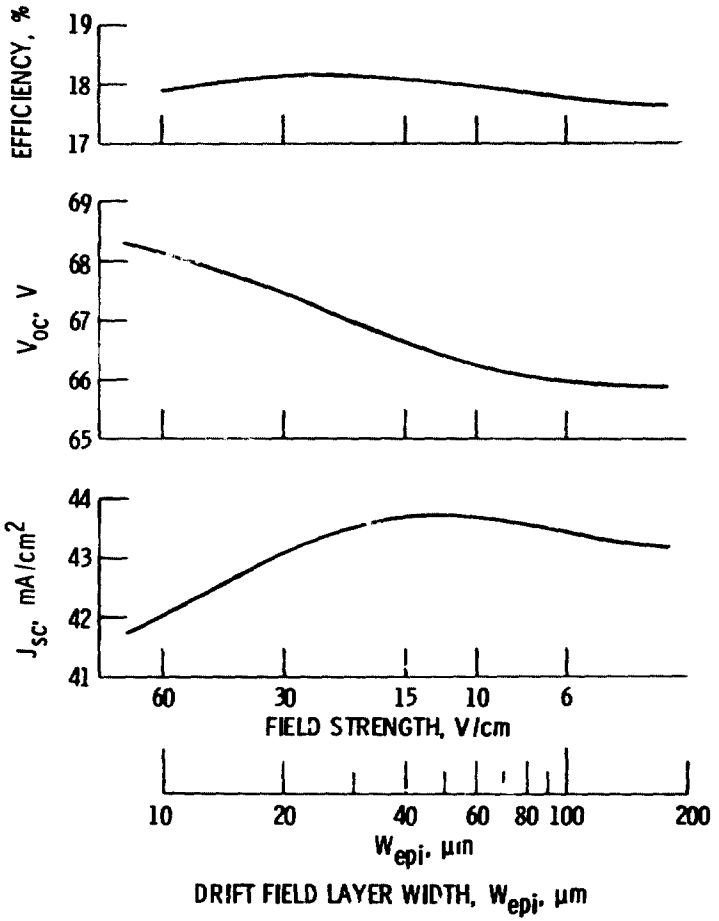

Figure 7. - Variation of performance with drift field layer width for the $N_{sub} = 10^{18}$, $N_{epi} = 10^{17}$ case.

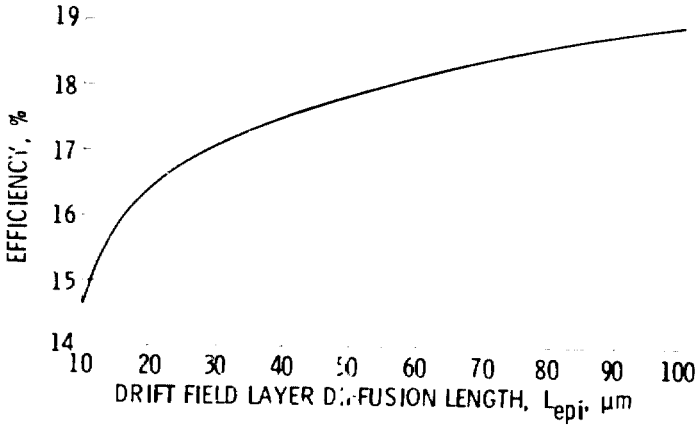

Figure 8. - Variation of efficiency with drift field layer diffusion length for $N_{sub} = 10^{18}$ cm^{-3}, $N_{epi} = 10^{17}$ cm^{-3} case.

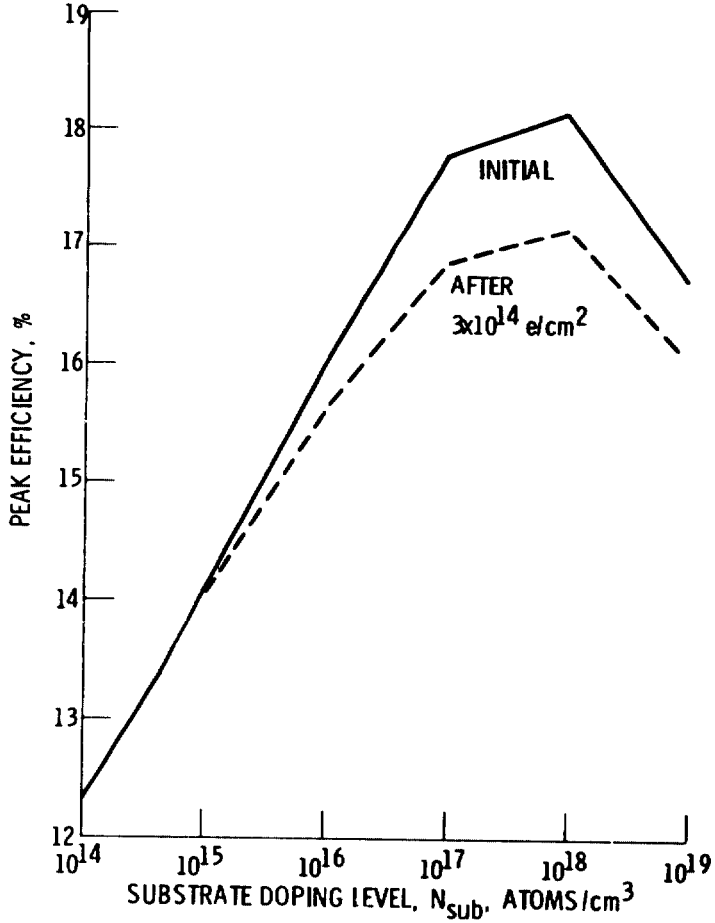

Figure 9. - Dependence of peak efficiency on substrate doping concentration.

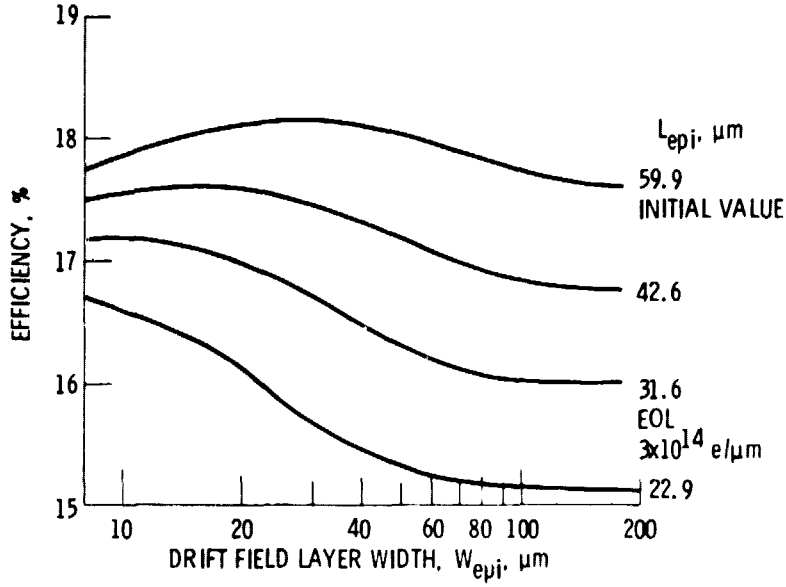

Figure 10. - Variation of efficiency with drift field layer width for values of diffusion length.